8th IFAC Symposium on Advanced Control of Chemical Processes
The International Federation of Automatic Control
Singapore, July 10-13, 2012

Closed-loop control of a SCR system using a NO_x sensor cross-sensitive to NH_3

A.Bonfils [⋆,†] **Y. Creff** [⋆] **O. Lepreux** [⋆] **N. Petit** [†]

[⋆] *IFP Energies nouvelles, Rond-point de l'échangeur de Solaize, BP 3, 69360 Solaize, France*
[†] *MINES ParisTech, Centre Automatique et Systèmes, Unité Mathématiques et Systèmes, 60 Bd St-Michel, 75272 Paris, Cedex 06, France*

Abstract: This paper presents a control strategy for an automotive selective catalytic reduction (SCR) system, for which the feedback is based on a NO_x sensor measurement. This NO_x sensor is cross-sensitive to NH_3, which is critical for control purposes: a study of the closed-loop dynamics is performed which permits to calibrate the control strategy. Experimental results illustrate the performance of the proposed approach.

Keywords: Automotive emissions; Diesel engines; NO_x sensor; Pitchfork bifurcation; Selective catalytic reduction, Cross-sensitivity

1. INTRODUCTION

Numerous recent technological developments have yielded substantial improvements in terms of NO_x emissions for diesel engines. Today, reducing NO_x emissions requires dedicated aftertreatment devices. Among the variety of encountered technologies, selective catalytic reduction (SCR) is one of the most appealing approach. Indeed, compared to its main alternative, which is the lean NO_x trap, SCR can treat larger amounts of NO_x. However, the (very) limited measurement possibilities and the complexity of the involved physico-chemical phenomena are critical issues that make control of SCR quite challenging.

The SCR systems considered in this paper uses ammonia (NH_3) as the reducing agent to convert NO_x inside a dedicated catalyst. In practice, NH_3 is generated by the decomposition of an urea solution. On the one hand, urea dosing is critical because an over-dosing can induce undesired release of NH_3 to the atmosphere (referred to as NH_3-slip) and generate extra-costs for the user. Tailpipe NH_3 emissions create unpleasant odors and are risky for human health. On the other hand, under-dosing results in insufficient NO_x reduction, and possible failure to meet emissions standards. To address these issues, control strategies can be used to manage the dosing of NH_3.

Recently, several SCR control strategies have been proposed, e.g. Upadhyay and van Nieuwstadt [2006], Schär et al. [2006], Hsieh and Wang [2009, 2010], where it has been proposed to control the amount of NH_3 stored in the catalyst (called NH_3 coverage (ratio) in this paper). For the purpose of applying such methodologies, an NH_3 coverage (ratio) observer based on NO_x sensors measurements must be developed. A particular difficulty is that available embedded NO_x sensors are cross-sensitive to NH_3 (Moos [2005]). This becomes critical when NH_3-slip is present downstream of the SCR catalyst. The aftereffects of their use in feedback control strategies have not been fully discussed so far. In this paper, this topic is addressed. The strategy we propose is to use the NO_x sensor measurement to estimate the NH_3 coverage ratio by a state observer. The estimate of the coverage ratio is dynamically forced by the control to track a setpoint (calculated for every operating conditions). Measurement errors induce observer bias, that can be limited by a proper choice of the gains, resulting from a scheduling methodology. Additionally, a mechanism is introduced to prevent large NH_3-slip that could result from misinterpretation of data produced by the sensor.

This paper is organized as follows. First, the SCR operation principle and the related control problem are presented. Then, the system and the sensor models are given, along with a control problem reformulation. In the sequel, a control strategy is proposed. The dynamics of the closed-loop system are studied, which leads to a simple calibration rule. Finally, representative experimental results are presented and show the good performances of this strategy.

2. SCR SYSTEM DESCRIPTION

2.1 Experimental setup

Fig. 1 illustrates the experimental setup under consideration in this study. The tested exhaust line is composed of a diesel oxidation catalyst (DOC), a Fe-ZSM-5 zeolite SCR catalyst, and a diesel particulate filter (DPF). The catalyst is 8 in long (L), has a diameter (D) of 2.5 in and an NH_3 storage capacity (Ω) of 70 mol/m^3. A dedicated injection system allows to control the flow of aqueous urea (AdBlue®). An estimation of the exhaust gas flow rate, the measurements of the inlet temperature sensor and of the two NO_x sensors are available in the control unit, as is pictured in Fig. 1. Moreover, testbench temperatures along the exhaust line, as well as two gas analysers are available for analysis purposes: a 5-gas analyser is located upstream

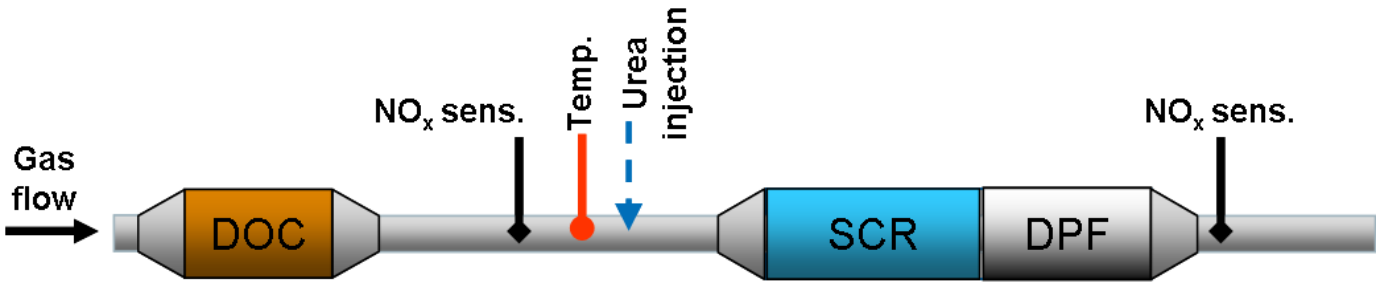

Fig. 1. Exhaust aftertreatment system of the considered experimental setup. Depicted sensors and actuator are used by the control strategy.

of the catalyst and a FTIR analyser (Fourier Transform InfraRed spectroscopy) downstream of the catalyst.

2.2 SCR catalyst

The SCR catalyst can be viewed as a tubular reactor fed by the exhaust gases coming from the diesel engine. This reactor consists of numerous thin channels which allow to maximize the mass transfer to the catalytic surface. Aqueous urea is injected at the reactor inlet. Urea is transformed into NH_3, which is stored (through an adsorption/desorption process) on the active phase of the catalyst (Ciardelli et al. [2004], Olsson et al. [2008]). The stored NH_3 catalytically reacts with NO_x. From this description, it appears that the NH_3 storage is the key parameter to control NO_x reduction efficiency. The interested reader can refer to Frobert et al. [2009] for further details. The main chemical reactions are described below.

NH_3 adsorption/desorption As discussed earlier, the NH_3 in gas phase is adsorbed on the SCR active surface. The adsorbed NH_3 can be desorbed from the substrate. It is represented by the surface coverage ratio, which is the ratio between the number of occupied catalytic sites and the total number of catalytic sites. Adsorption and desorption are complex phenomena that require tedious modeling and calibration efforts. For the most part, they are out of the current scope of our studies.

The direct oxidation of adsorbed NH_3 by oxygen is not presented because it has no impact on the closed-loop analysis. However, adaptation is straightforward.

NO_x reduction The adsorbed NH_3 reacts with NO_x (and possibly oxygen from the exhaust gas) to produce nitrogen and water. In this study, NO and NO_2 are lumped into the total amount of NO_x.

Operating conditions The system is operated in highly transient conditions. Variations of the exhaust gas flow, the temperature, and the amount of NO_x, respectively, range from 25 to 250 kg/h, 100 to 400 °C, and 10 to 350 mole ppm.

2.3 NO_x sensors & system open loop steady state behavior

The study of the system open loop (stable) behavior helps to understand the control issue. In Fig. 2, the steady state values of z_1 (outlet NO_x) and z_2 (outlet NH_3) are represented as a function of u (inlet NH_3 injection), and are

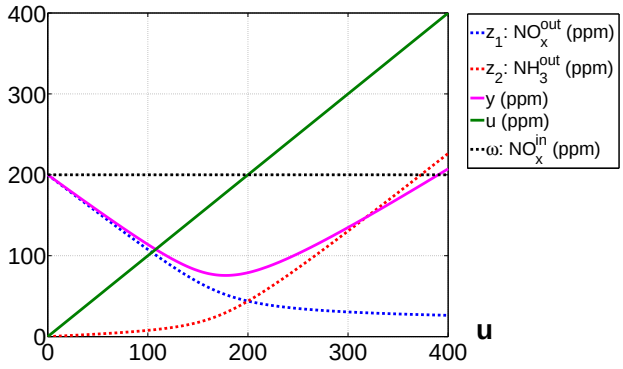

Fig. 2. Outlet NO_x sensor response to increasing NH_3 injection at the inlet of the catalyst (steady state). The temperature, the gas flow rate and the NO_x inlet concentration are respectively set to 300 °C, 100 kg/h and 200 mole ppm.

compared against the outlet measurement y. It is shown that while u is increased, z_1 decreases (NO_x are reduced) and z_2 increases (NH_3-slip increases). The measurement y delivered by the NO_x sensor located downstream of the catalyst is (with a good level of accuracy) a linear combination of z_1 (NO_x) and z_2 (NH_3) (see Moos [2005] for details on the operation principle). As a result, y is non monotonic: it is close to z_1 when z_2 is small, but largely corrupted when z_2 becomes significant (i.e. NH_3-slip becomes overwhelming). One can easily figure out that this behavior can be troublesome for feedback control purposes.

The inlet NO_x sensor measurement is not polluted by NH_3 since it is located upstream of the injector.

2.4 Problem Formulation

A control problem of interest for the SCR system consists of managing the injection of the urea solution in order to maximize the NO_x conversion while maintaining release of NH_3 within acceptable levels (peaks limited to 30 mole ppm, average value less than 10 mole ppm). The system evolves in an environment where the temperature, the gas flow and the amount of NO_x are variable and measured. To achieve the formulated objectives, closed-loop control based on NO_x sensor feedback can be employed. However, as will appear, the NH_3 cross-sensitivity of the NO_x sensor limits the performance of such a control strategy.

3. INPUT OUTPUT DESCRIPTION

3.1 Initial model

Upadhyay and van Nieuwstadt [2006], Devarakonda et al. [2009] consider a model obtained by material balances for two species with three states: NH_3 and NO_x in gas phase, as well as adsorbed NH_3

$$\begin{cases} \dot{x} &= k_a z_2 (1-x) - k_d x - k_r z_1 x \\ \dot{z_1} &= \dfrac{v}{L}(\omega - z_1) - \Omega k_r z_1 x \\ \dot{z_2} &= \dfrac{v}{L}(u - z_2) - \Omega k_a z_2 (1-x) + \Omega k_d x \end{cases} \quad (1)$$

where x is the NH_3 coverage ratio. z_1 and z_2 are the NO_x and the NH_3 outlet gas concentrations. The input u is the NH_3 inlet concentration, and ω is a known and bounded disturbance, the NO_x inlet concentration. All these concentrations are expressed in mol/m^3. Respectively, k_a (in m^3/mol/s), k_d (in s^{-1}) and k_r (in m^3/mol/s) are the reaction rate of adsorption, desorption and NO_x reduction (defined by Arrhenius laws). L is the length of the catalyst (in m), v is the gas velocity (in m/s), and Ω is the NH_3 storage capacity (in mol/m^3).

The NO_x sensor located downstream of the catalyst delivers an information corrupted by the NH_3 outlet concentration. This sensor can be modeled with a good level of confidence as (Hsieh and Wang [2011])

$$y = z_1 + \alpha z_2 \quad (2)$$

In this study, α is considered to be a constant value equal to 0.8.

3.2 Model reduction

To start the analysis, a model reduction is performed. Consider system (1) where each equation is multiplied by $\epsilon = L/\Omega$ (typically $\epsilon \approx 3.10^{-3}$). In the singular perturbation form (Khalil [2002]), one obtains

$$\begin{cases} \dot{x} &= f(x,z,u,\omega) \quad \text{(slow)} \\ \epsilon \dot{z} &= g(x,z,u,\omega) \quad \text{(fast)} \end{cases} \quad (3)$$

where $z = (\, z_1 \;\; z_2 \,)'$. For any given x, the fast dynamic equation is asymptotically stable, and $g(x,z,u,\omega) = 0$ has a unique solution.

$$z = h(x,\omega,u) = \begin{pmatrix} h_1(x,\omega) \\ h_2(x,u) \end{pmatrix} \quad (4)$$

where $h_1(x,\omega) = \dfrac{\omega}{1 + k_r x/\gamma}$, $h_2(x,u) = \dfrac{u + k_d x/\gamma}{1 + k_a(1-x)/\gamma}$ and $\gamma = \dfrac{v}{L\Omega}$. The system (1) can be reduced to its slow dynamics

$$\begin{cases} \dot{x} &= f(x, h(x,\omega,u), u, \omega) \\ &= \gamma\,(u + h_1(x,\omega) - h_2(x,u) - \omega) \end{cases} \quad (5)$$

This reduction is valid for all positive times because (5) is asymptotically stable.

This reduction stresses the SCR control problem as a problem bearing on the coverage ratio x, only.

3.3 Problem reformulation

From this, one can reformulate the control problem with the SISO dynamics

$$\begin{cases} \dot{x} &= \gamma\,(u + h_1(x,\omega) - h_2(x,u) - \omega) \\ y &= h_1(x,\omega) + \alpha h_2(x,u) \end{cases} \quad (6)$$

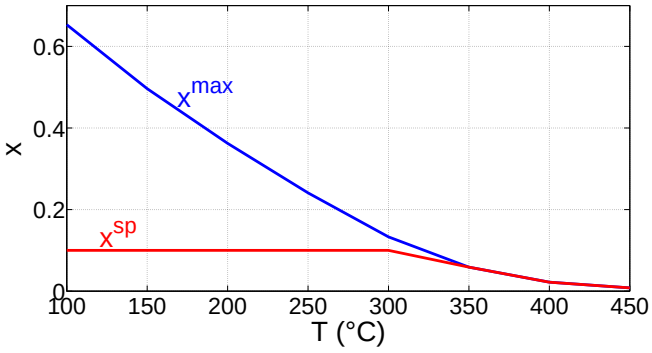

Fig. 3. Maximum coverage ratio with 10 mole ppm of NH_3-slip ($x^{\max}$) and setpoint map (x^{sp}) as functions of temperature.

Then, because it is not directly measured, controlling the coverage ratio x requires to design an observer to provide an estimation $\hat{x}$ that is controlled to the setpoint x^{sp}.

First, let us explain how x^{sp} is determined, based on the following considerations. Maintaining large values of x allows to reach high levels of NO_x reduction efficiency, but increases the NH_3-slip. To this purpose, values of x implying 10 mole ppm of NH_3-slip at steady state are computed from system (1). In Fig. 3, these values (denoted $x^{\max}$) are reported as a function of the temperature only. Indeed, temperature plays the most significant role among the parameters. Then, x^{sp} should not be chosen greater than $x^{\max}$. Moreover, to prevent large NH_3-slip during transients of temperature, x^{sp} is limited to a lower value (typically 0.1) for low temperatures (with very slight detrimental impact on the efficiency). This limit corresponds to the possibility for the setpoint to be tracked during a fast rise in temperature. Indeed, x can be only decreased slowly at constant temperature (by ω, see (6) with u saturated to 0), while rises in temperature imply fast decreases of $x^{\max}$ (see Fig. 3).

The proposed observer is defined as

$$\begin{aligned} \dot{\hat{x}} &= \ell(u, y(x,\omega,u), \hat{x}, \omega) \\ &= \gamma\,(u + y - \omega) - k_L\,(\hat{x} - x^{\text{c}}) \end{aligned} \quad (7)$$

where k_L is the observer gain. Implicitly, in this observer design derived from (6), h_2 is neglected because the NH_3-slip is neglected and h_1 is directly replaced by the measurement y. In (7), y is used to calculate a tentative value x^{c} of the coverage, as

$$x^{\text{c}} = h_1^{-1}(y,\omega) \quad (8)$$

As y is not invertible with respect to x, one shall note that only the (dominant) part h_1 is inverted in (8) (NH_3-slip is neglected) and x^{c} is calculated with the two NO_x sensors signals. This strong simplification yields the mapping represented in Fig. 4. In this figure, for most of the values of the interpreted coverage x^{c}, the true coverage x can take two distinct values. Out of those two, the desired one is

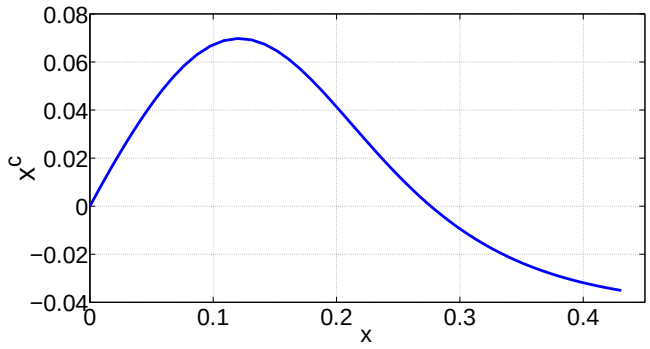

Fig. 4. Interpreted coverage x^{c} as a function of x, for some constant values of v and ω (taken at equilibrium).

the smallest. The real control design problem is to know, for a given x^{c}, which value of x has to be considered in the feedback strategy. The control law proposed in the next section addresses this issue.

4. CONTROL STRATEGY

In this section, the control strategy is introduced, as well as an analysis of the closed-loop dynamics, that gives clues to calibrate the observer gain k_L.

4.1 Proposed control strategy

The control strategy is designed to force $\dot{\hat{x}} = -k_P\,(\hat{x} - x^{\mathrm{sp}})$. The linearizing feedback law is saturated for negative values to account for the actuator limitations. This yields

$$\begin{aligned} &u - \max(0, \omega - y + \frac{1}{\gamma}\left[k_L\,(\hat{x} - x^{\mathrm{c}}) - k_P\,(\hat{x} - x^{\mathrm{sp}})\right]) \\ &\triangleq \Phi(y(x,\omega,u),\hat{x},\omega) = 0 \end{aligned} \tag{9}$$

The closed-loop system consisting of (6), (7) and (9) is

$$\begin{cases} \dot{x} &= f(x, h(x,\omega,u), u, \omega) \\ \dot{\hat{x}} &= \ell(u, y(x,\omega,u), \hat{x}, \omega) \\ 0 &= \Phi(y(x,\omega,u),\hat{x},\omega) \end{cases} \tag{10}$$

4.2 Description of closed loop equilibria

The equilibria of the preceding dynamics always satisfy $\hat{x} = x^{\mathrm{sp}}$. Then, $\partial f/\partial k_P$ and $\partial \ell/\partial k_P$ are null at these points. Generally, the system has one or three equilibrium points, which solely depend on the value of k_L. Stability is studied using the triangular form of the Jacobian of the closed loop dynamics, obtained through the implicit function theorem applied to the algebraic equation defining u. On the domain of interest for the variables ω, x^{sp}, T, v, the system presents a pitchfork bifurcation when the parameter k_L is varied. The system switches from one stable node to the other are possible but undesirable. In Fig. 5, all the equilibria are represented for different k_L, $T = 250$ °C, $\omega = 200$ mole ppm, $v = 4.5$ m/s and $x^{\mathrm{sp}} = 0.1$. For a small k_L, there is only one stable equilibrium point close to the setpoint. This is the desired equilibrium. When k_L is increased, two more points appear. The first equilibrium (desired) is stable, the second one is unstable and the last one, which corresponds to a very high coverage, is stable too. Fig. 5 reports the existence of an upper bound for k_L (denoted k_L^{lim}), from which the desired equilibrium point is no longer stable. Slightly below this critical value, the second equilibrium becomes stable.

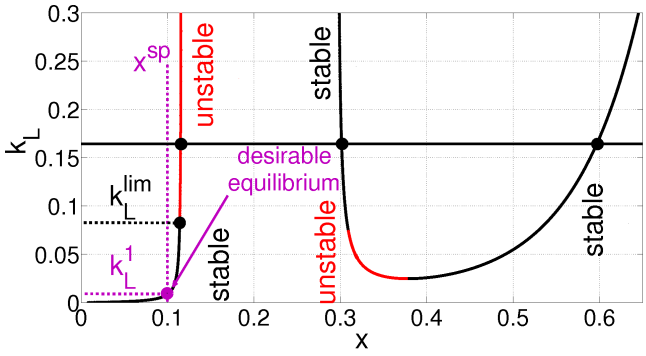

Fig. 5. Equilibria of the closed loop dynamics (10) as function of k_L. The stable equilibrium points are represented in black and the unstable ones in red.

4.3 NO_x measurement interpretation: detection of NH_3-slip

The closed loop dynamics (10) asymptotically reaches one of the stable equilibria, out of which only the smallest one is of interest, as already discussed. Fortunately, being in the vicinity of one undesirable equilibria can be easily detected thanks to the downstream NO_x sensor, without any risk of misinterpretation. Indeed, when $x^{\mathrm{c}} < 0$, the measurement of the inlet sensor is lower than the measurement at the outlet. In the measurement y, it is clear that the part h_2 is overwhelming the useful signal h_1. With certainty, the sensor measures NH_3. This region of NH_3-slip detection is pictured in Fig. 6. When this occurs, the following actions are carried out. First, the observer state $\hat{x}$ is set to the maximum coverage ratio before NH_3 desorption of 10 mole ppm. This coverage is taken from the *a priori* $x^{\max}$ map presented in Fig. 3. Meanwhile, u is set to zero, which stops the NH_3 injection. Finally, injection is kept null as long as $\hat{x}$ is greater than x^{sp}.

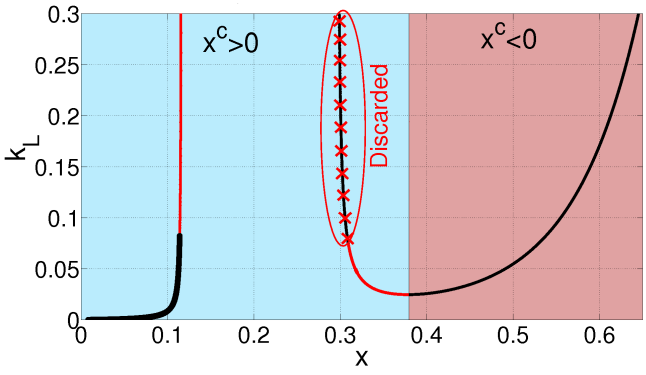

Fig. 6. Equilibria of the closed loop dynamics (10) as function of k_L. The region where NH_3-slip is detected ($x^{\mathrm{c}} < 0$) is is pictured in red and the one where it is not detected ($x^{\mathrm{c}} > 0$) in blue. The undesirable points discarded by the implementation (11) of the closed loop are represented.

4.4 Discarding the remaining undesirable stable equilibrium

The proposed feedback controller is implicit. A possible explicit implementation in discrete time is as follows (where Δ is the sampling period):

$$\begin{cases} x_{k+1} = x_k + \Delta f(x_k, h(x_k, \omega_k, u_k), u_k, \omega_k) \\ \hat{x}_{k+1} = \hat{x}_{k+1} + \Delta \ell(y_k(x_k, \omega_k, u_k), \hat{x}_k, \omega_k) \\ u_{k+1} = \max\Big(0, \omega_k - y_k(x_k, \omega_k, u_k) + \\ \qquad \frac{1}{\gamma}\left[k_L\left(\hat{x}_{k+1} - x_k^{\mathrm{c}}\right) - k_P\left(\hat{x}_{k+1} - x_k^{\mathrm{sp}}\right)\right]\Big) \end{cases} \tag{11}$$

Interestingly, this discrete time dynamics is unstable for every value of the second stable equilibrium. As a result, this troublesome point is discarded by the implementation of the proposed closed loop controller. Combined with the previous detection method, this implementation provides convergence to the equilibrium of interest.

4.5 Gain scheduling methodology

Choosing the value for k_L is decisive because it defines the value of the reached equilibrium. The most relevant value for this gain would be k_L^1 (see in Fig. 6) because it corresponds to x^{sp}. But to account for model uncertainty, the gain k_L can be simply scheduled to provide acceptable performance. An off-line study reveals that k_L can be taken as a piecewise affine function of w, which leads to values that are valid for the ranges defined in Section 2 and induces acceptable coverage bias in the coverage variable x:

$$\begin{cases} k_L = 0 & , \quad \omega < 10 \text{ mole ppm} \\ k_L = \omega\beta & , \quad 10 < \omega < 100 \text{ mole ppm} \\ k_L = 100\beta & , \quad \omega > 100 \text{ mole ppm} \end{cases} \tag{12}$$

where β is a calibration parameter that may depend on temperature. Experimental results using this calibration are reported and discussed in the next section.

5. EXPERIMENTAL RESULTS

In this section, to illustrate the proposed approach, a fully instrumented vehicle is mounted on a roller test bench and tested under real driving conditions. First, to argue

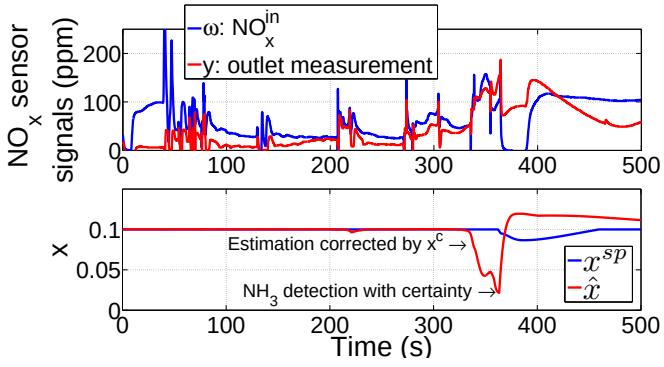

Fig. 7. Case of a poorly tuned k_L under transient conditions: evolution of ω, y, x^{sp} and $\hat{x}$ as functions of time. Experimental results.

the necessity of scheduling the gain k_L, a test is performed with a poorly tuned k_L. As appears in Fig. 7, this strategy has relatively limited performance. This clearly means that a proper choice of k_L is crucial, as well as good detection of NH_3-slip. Fig. 7 presents the evolution of (ω,y) and $(x^{\mathrm{sp}},\hat{x})$. At about $t = 330$ s, $\hat{x} - x^{\mathrm{c}}$ increases (due to the cross-sensitivity to NH_3, the apparent efficiency calculated from the NO_x sensors decreases): $\hat{x}$ decreases, and u is increased. This results in significant NH_3-slip, as can be seen from traces of ω and y. At last, when NH_3 is detected with certainty, the coverage ratio is corrected, and the injection is turned off ($u = 0$).

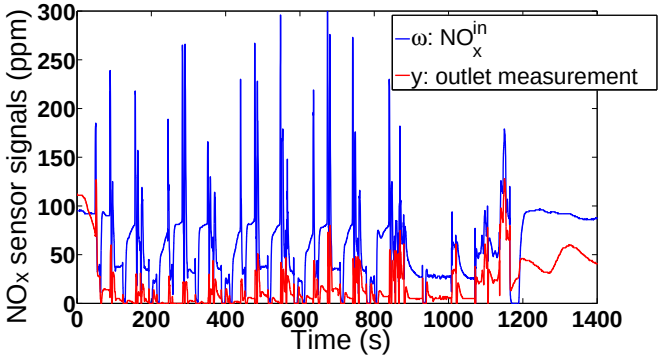

(a) NO_x emissions.

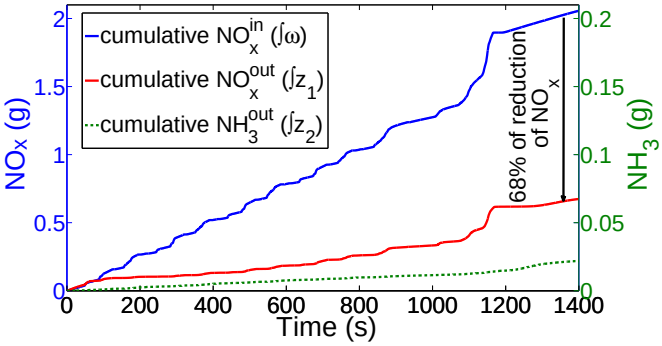

(b) Cumulative NO_x and NH_3 emissions.

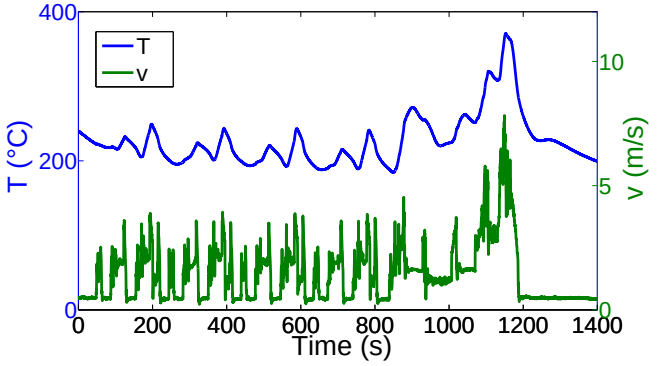

(c) Variation of temperature and gas velocity during the cycle.

Fig. 8. Warm start NEDC cycle. Experimental results.

On the other hand, we now use the proposed gain scheduling method and perform a NEDC cycle (to check the fulfillment of Euro standards) with a warm start. The results are presented in Fig. 8.

This test was run with a catalyst initially empty at the start of the cycle. Fig. 8a and Fig. 8b report instantaneous and cumulative amounts of NO_x, produced by the engine and released to the atmosphere, respectively. Changes of

the temperature and the gas velocity during the cycle are illustrated in Fig. 8c. In this test, the control strategy performance is satisfactory, both in terms of NO_x reduction and NH_3-slip limitation. Indeed, the reduction efficiency is about 68 % while a very low amount of NH_3 is detected by the FTIR analyzer. NH_3 average concentration is 3 mole ppm over the cycle and 20 mole ppm maximum, which is below usually acceptable limits.

6. CONCLUSION

In this paper, a control strategy for a selective catalytic reduction (SCR) system has been described. It consists of an observer and a tracking loop. It controls the NH_3 coverage ratio and allows one to mitigate the trade-off between NO_x conversion efficiency and tailpipe NH_3-slip. In this strategy, the NH_3 coverage ratio is estimated using the measurement of a commercial NO_x sensor located downstream of the catalyst. This sensor is cross-sensitive to NH_3. It is shown that this cross-sensitivity can make the closed-loop system converge to an undesirable value of the coverage ratio as new equilibrium points are created by the feedback loop. The additional and undesirable setpoints are either discarded by the discrete time implementation of the control strategy (which makes them unstable) or detected with certainty from the available data. A parametric study is performed and shows how the observer gain has to be tuned so that the system can remain at all times in the vicinity of the setpoint of interest. As a result, the strategy leads to good performance, as has been demonstrated in a roller testbench under real transient conditions.

REFERENCES

C. Ciardelli, I. Nova, E. Tronconi, B. Konrad, D. Chatterjee, K. Ecke, and M. Weibel. SCR-denox for diesel engine exhaust aftertreatment: unsteady-state kinetic study and monolith reactor modelling. *Chemical Engineering Science*, 59(22-23):5301–5309, 2004. ISCRE18.

M. Devarakonda, G. Parker, J. H. Johnson, and V. Strots. Model based control system design in a urea-SCR aftertreatment system based on NH_3 sensor feedback. *International Journal of Automotive Technology*, 10(6): 653–662, 2009.

A. Frobert, Y. Creff, S. Raux, C. Charial, and A. Audouin. SCR for passenger car: The ammonia-storage issue on a Fe-ZSM-5 catalyst. In *SAE International*, number 2009-01-1929. SAE International, 2009.

M. F. Hsieh and J. Wang. Backstepping based nonlinear ammonia surface coverage ratio control for diesel engine selective catalytic reduction systems. In *ASME Conference Proceedings*, number 48920, pages 889–896. ASME, 2009.

M. F. Hsieh and J. Wang. Staircase ammonia coverage ratio profile control for diesel engine two-cell Selective Catalytic Reduction systems. In *Proc. American Control Conference*. IEEE, 2010.

M. F. Hsieh and J. Wang. Development and experimental studies of a control-oriented SCR model for a two-catalyst SCR system. *Control Engineering Practice*, 19 (4):409–422, 2011.

H. K. Khalil. *Nonlinear systems (third edition)*, volume 3. Prentice Hall, 2002.

R. Moos. A brief overview on automotive exhaust gas sensors based on electroceramics. *Int. Journal of Applied Ceramics Technology*, 2(5):401–413, 2005.

L. Olsson, H. Sjövall, and R. J. Blint. A kinetic model for ammonia selective catalytic reduction over Cu-ZSM-5. *Applied Catalysis B: Environmental*, 81(3-4):203–217, 2008.

C. M. Schär, C. H. Onder, and H. P. Geering. Control of an SCR catalytic converter system for a mobile heavy-duty application. *IEEE Transactions on Control Systems Technology*, 14(4):641–653, 2006.

D. Upadhyay and M. J. van Nieuwstadt. Model based analysis and control design of a urea-SCR DeNOx aftertreatment system. *Journal of Dynamic Systems, Measurement, and Control*, 128(3):737–741, 2006.